

Landscape biogeochemistry reflected in shifting distributions of chemical traits in the Amazon forest canopy

Gregory P. Asner^{*}, Christopher B. Anderson, Roberta E. Martin, Raul Tupayachi, David E. Knapp and Felipe Sinca

Tropical forest functional diversity, which is a measure of the diversity of organismal interactions with the environment, is poorly understood despite its importance for linking evolutionary biology to ecosystem biogeochemistry. Functional diversity is reflected in functional traits such as the concentrations of different compounds in leaves or the density of leaf mass, which are related to plant activities such as plant defence, nutrient cycling, or growth. In the Amazonian lowlands, river movement and microtopography control nutrient mobility, which may influence functional trait distributions. Here we use airborne laser-guided imaging spectroscopy to develop maps of 16 forest canopy traits, throughout four large landscapes that harbour three common forest community types on the Madre de Dios and Tambopata rivers in southwestern Amazonia. Our maps, which are based on quantitative chemometric analysis of forest canopies with visible-to-near infrared (400–2,500 nm) spectroscopy, reveal substantial variation in canopy traits and their distributions within and among forested landscapes. Forest canopy trait distributions are arranged in a nested pattern, with location along rivers controlling trait variation between different landscapes, and microtopography controlling trait variation within landscapes. We suggest that processes of nutrient deposition and depletion drive increasing phosphorus limitation, and a corresponding increase in plant defence, in an eastward direction from the base of the Andes into the Amazon Basin.

Lowland Amazonian forest communities occupy an area of more than five million square kilometres, stretching from the Atlantic coast to the foothills of the Andes. Thousands of tree species are found throughout these communities, which often differ floristically in response to the underlying geologic substrate, regional climate, and other abiotic factors¹. Yet, despite more than a century of field research on the floristic composition of Amazonian forests, relatively little is known about their functional diversity. Here we use Tilman's² definition of functional diversity as the range and value of the traits of organisms that influence ecosystem functioning. Specifically, we have a poor understanding of whether shifts such as those observed in community-scale floristic composition (beta diversity) also occur for functional diversity. If functional shifts do occur in spatially explicit patterns, they would express critical variation in biogeochemical processes, including carbon and nutrient cycling, and potential variation in forest responses to climate change³.

Previous studies have found evidence for landscape-scale variation in Amazonian forest functional diversity. For example, pedogenetically distinct substrates are linked to differences in leaf defence against pests and pathogens⁴. Trade-offs in foliar allocation to growth and defence compounds are also observed at transitions from older *terra firme* to younger floodplain soils⁵. Field plots and models of pan-Amazonian functional traits have also suggested basin-wide variation in canopy responses to broad climatic and geologic controls^{6,7}. However, within any given forest community, foliar traits vary phylogenetically⁸, which challenges field studies to sample sufficiently to resolve intra- and inter-community patterns. Field surveys⁸, field manipulations⁴ and remote sensing have not provided spatial distributions of plant functional traits within and across communities or landscapes.

This problem of understanding canopy functional distributions in lowland Amazonia is acute throughout its southwestern forests, where a complex mosaic of geologically and hydrologically diverse surfaces underlies the canopy⁹. With the rise of the Andes since the Miocene, rivers flowed eastwards, eventually draining into the Amazon river¹⁰. Today, surface substrates switch from those dominated by erosional processes at the Andes to vast depositional surfaces of widely varying age to the east. In the southwestern Amazon, lowland depositional areas of mostly Quaternary and Neogene age form terraces or *terra firme*. Rivers incise and erode these terraces, creating floodplains of variable size dating to the Holocene, with terrace–floodplain elevation differences decreasing eastwards from the Andes, and well into Brazil¹¹. These patterns represent variation in lowland microtopography that affects water availability, nutrient mobility and resource accumulation¹². Here we define lowland Amazonian microtopography as variation in elevation of less than 25 m, and often less than 5 m (ref. 13). Through its role in mediating hydrologic conditions and substrate nutrient distributions, we hypothesize that microtopography filters forest canopy functional traits expressing spatially explicit changes in the fundamental biogeochemical properties of lowland tropical forests. The role of microtopography in sorting tropical functional trait distributions has not been determined spatially because the scales of variability—from local to regional levels—are difficult to measure.

Canopy chemistry

Canopy chemistry is an important component of plant functional trait diversity that mediates carbon and nutrient cycling under varying environmental conditions. Chlorophylls and carotenoids are synthesized in foliage to capture solar radiation and to mitigate photodamage. Nitrogen (N) supports light capture and carbon (C)

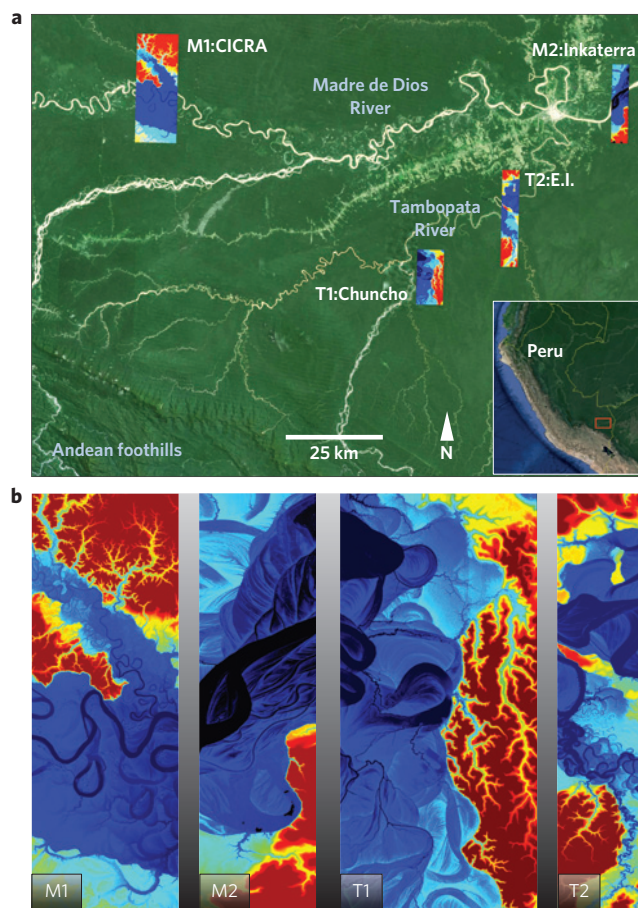


Figure 1 | Four lowland Amazonian study landscapes totalling more than 37,000 ha on two rivers. **a**, Landscapes M1:CICRA and M2:Inkaterra are on the Madre de Dios River. Landscapes T1:Chuncho and T2:Explorers Inn (E.I.) are on the Tambopata River. The inset map indicates the study region in southwestern Amazonia. **b**, Close-up views of digital terrain models derived from airborne LiDAR for each study landscape. Blue colours indicate late Holocene alluvium (inceptisols) underlying floodplain and swamp forests. Yellow-to-red colours indicate higher-elevation Pleistocene terraces (ultisols) underlying *terra firme* forests. See Supplementary Table 1 for landscape details.

fixation. Other macronutrients from rock-derived sources, such as phosphorus (P), calcium (Ca), magnesium (Mg) and potassium (K), regulate growth, allocation and cell structure¹⁴. Secondary micronutrients, such as boron (B) and iron (Fe), mediate further metabolic processes. Carbon fixation generates non-structural carbohydrates (sugars, starches, pectin), hereafter referred to as soluble C, which may subsequently be transformed into cellulose and lignin to support cell wall structure and defend against herbivory¹⁵. Polyphenols, hereafter referred to as phenols, are also synthesized for chemical defence, which is important in tropical forests subject to high pest and pathogen pressure¹⁶. The overall foliar investment strategy is expressed in leaf mass per unit area (LMA), which also affects foliar water content¹⁷.

As fundamental as plant chemical traits are to understanding ecosystem functioning and biogeochemical processes, we know little about their spatial distribution in tropical regions such as lowland Amazonia. Here we developed the first high-resolution remotely sensed maps of multiple canopy chemical traits in lowland Amazonia. A new remote sensing technique using airborne high-fidelity imaging spectroscopy (HiFIS; also known as hyperspectral imaging) fused with LiDAR (light detection and ranging)¹⁸ was applied over four large forested landscapes on microtopographically

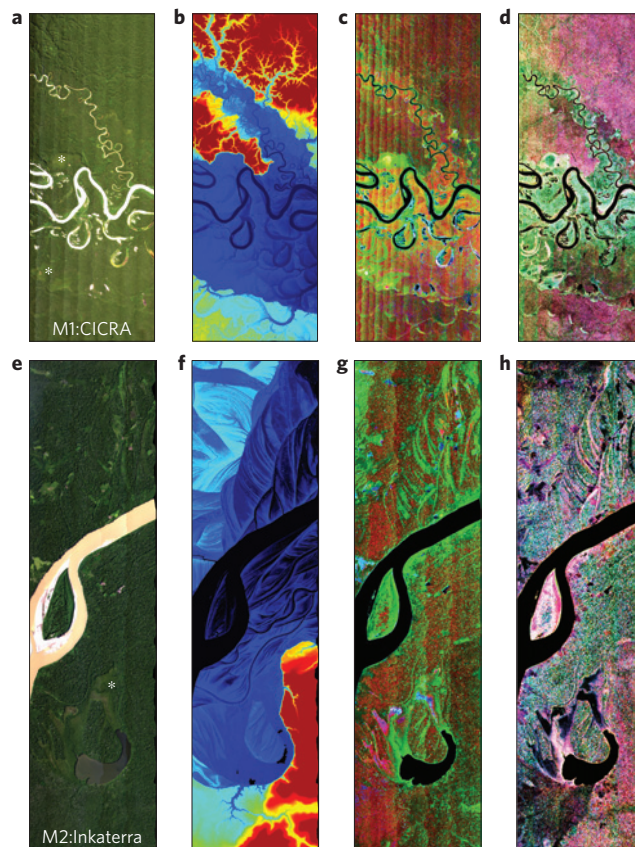


Figure 2 | Remote sensing of multiple canopy chemical traits across two Amazonian landscapes. **a, e**, Natural colour images of landscapes. **b, f**, Digital terrain models delineating floodplains in blue from *terra firme* in yellow-red. **c, g**, Colour composite of remotely sensed foliar Ca (red), P (green) and Mg (blue). **d, h**, Colour composite of remotely sensed lignin (red), soluble C (green) and cellulose (blue). Variation in illumination and viewing angles cause image striping, with little effect on chemical estimates. Asterisks mark locations of swamp forest. The landscapes shown are M1:CICRA (**a–e**) and M2:Inkaterra (**f–h**); other study landscapes are shown in Supplementary Fig. 1.

contrasting reaches of two lowland Amazonian river systems, at a mapping resolution of 2 m and a reporting resolution of 1 ha. We chose the landscapes because each contains the three most common forest types found in western Amazonia—floodplain, terrace (*terra firme*) and swamp—and because of their contrasting position along two major rivers draining the Andes (Fig. 1 and Supplementary Table 1). We used the maps to determine whether variation in microtopography affects plant functional trait distributions within landscapes, and to assess regional-scale (inter-landscape) differences in canopy functional traits along rivers in the Amazonian lowlands.

Within-landscape patterns

We found that microtopography imparts a strong spatial pattern in multiple canopy chemical traits within each mapped Amazonian landscape (Figs 2 and 3 and Supplementary Fig. 13). Spatial distributions of rock-derived macronutrients (P, Ca, Mg) indicated much higher average concentrations in floodplain canopies than in terrace canopies (Fig. 4a and Supplementary Table 2). Floodplain canopies exhibited lower investment in lignin and increased allocation to soluble C relative to terrace canopies. However, these terrace–floodplain differences ($3–11 \pm 0.05–0.2\%$) were much smaller than those observed for P, Ca and Mg ($9–117 \pm 0.1–2\%$) (Fig. 4a). Other canopy chemical traits, including

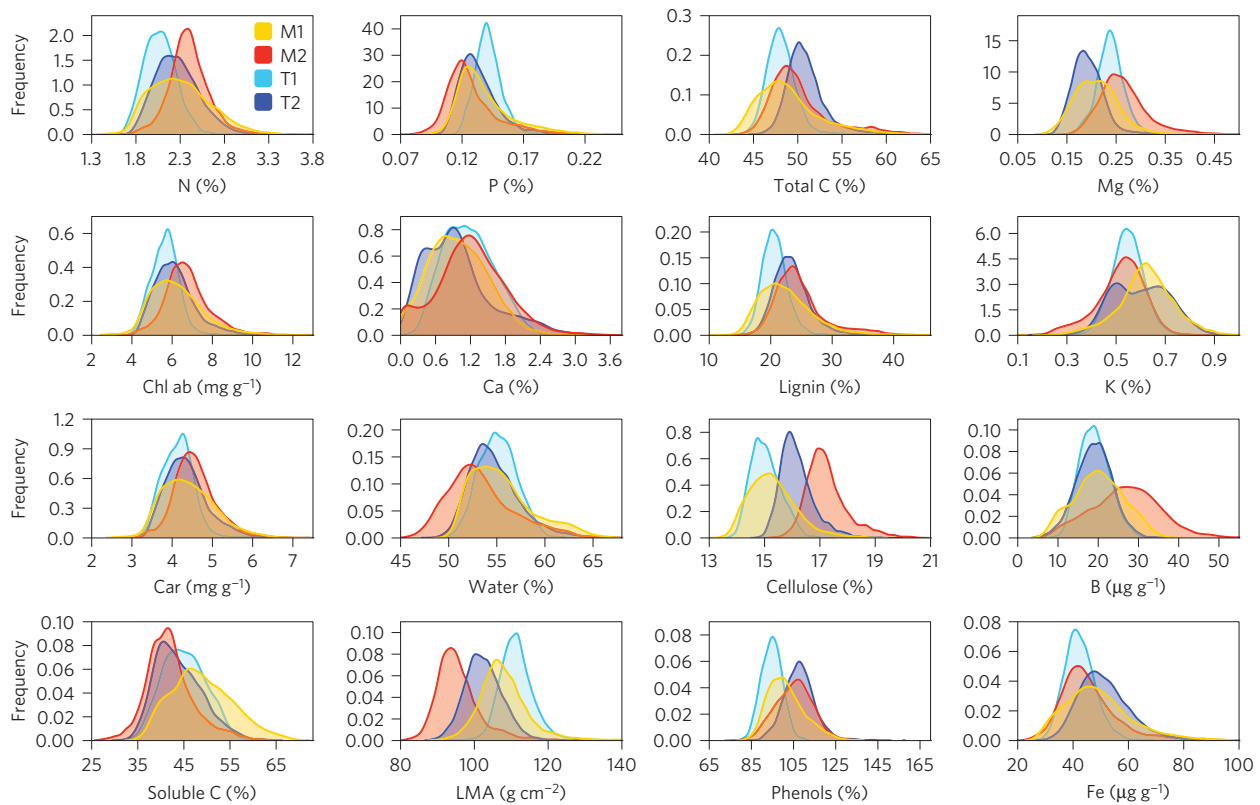


Figure 3 | Spatial distributions of remotely sensed canopy traits in floodplain forests on four lowland Amazonian landscapes. Referring to Fig. 1, M1 and M2 are the upriver (CICRA) and downriver (Inkaterra) landscapes, respectively, on the Madre de Dios River. T1 and T2 are the similar pair (Chuncho, E.I.) on the Tambopata River. Additional trait distributions are provided for terrace and swamp forests in Supplementary Figs 2 and 3. These data are reported at 1-ha mapping resolution.

N, photosynthetic pigments, cellulose and phenols showed weaker or inconsistent differences between neighbouring floodplain and terrace communities.

Occupying the floodplains in some lower-lying areas, swamp forests dominated by *Mauritia flexuosa* exhibited highly unique chemical trait distributions compared to neighbouring floodplain tree canopies (Fig. 4b and Supplementary Fig. 3 and Supplementary Table 2). In all four landscapes, swamp forest canopies invested much less in light capture and growth chemicals—including N, photosynthetic pigments, Ca and K—than did neighbouring floodplain canopies. By contrast, swamp canopies invested much more in P, water, soluble C, and all structural and defensive foliar traits (lignin, cellulose, phenols). LMA was also consistently higher and foliar B was much lower in swamp than in comparable floodplain canopies.

Inter-landscape patterns

Taking into account the distributions of mapped traits (Fig. 3 and Supplementary Figs 2–3), we assessed the relative importance of each forest type within landscapes, compared to the position of each landscape along rivers, in explaining regional variation in canopy chemical traits (Table 1). Comparing terrace and floodplain forests across all four study regions (without palm forests), landscape position emerged as far more important than forest type in determining foliar concentrations of light capture and growth chemicals, including N, chlorophylls, carotenoids and soluble C. Similarly, leaf structure and defence chemistry was much more closely related to landscape position than to forest type. Total C, lignin, cellulose and phenol distributions were shifted to lower concentrations in upriver landscapes compared to their downriver counterparts (Supplementary Table 2).

Relative to the dominant role of landscape position on light capture, growth, structural and defence chemistry, rock-derived macronutrients, including P, Ca and Mg, were more closely associated with forest type than landscape position along rivers (Table 1). There was a strong interaction between landscape position and forest type in explaining P, K and Mg—a pattern only weakly observed for most other canopy chemicals. Despite differences in the distance between landscapes along each river (Fig. 1), foliar N consistently increased and P decreased in downriver floodplain and terrace forests (Fig. 4c,d). Moreover, LMA consistently decreased, whereas total C, lignin, cellulose and phenols increased downriver in both terrace and floodplain forests (Supplementary Table 2). By contrast, base cations, soluble C and photosynthetic pigments showed variable responses to landscape position. However, after including swamp forests in the analysis, forest type became much more important than landscape position in explaining variation in light capture and growth traits (Table 1). Similarly, the role of forest type in explaining rock-derived nutrient concentrations, and structural and defence compound chemistry, increased sharply when including swamp forest in the analyses. These results emphasize the unique biochemistry of swamp forests in lowland Amazonia, independent of their position along rivers.

Functional trait distributions

Our results suggest that lowland Amazonian forest canopies are arranged in a chemically nested pattern, with one scale of variation mirroring microtopography within landscapes, and another changing with landscape position along rivers (Fig. 5). Compared to terrace forests, floodplain canopies maintain higher concentrations of P, Ca and Mg in their leaves (Fig. 5a). Lignin, which contributes to physical defence, is found in statistically lower concentrations

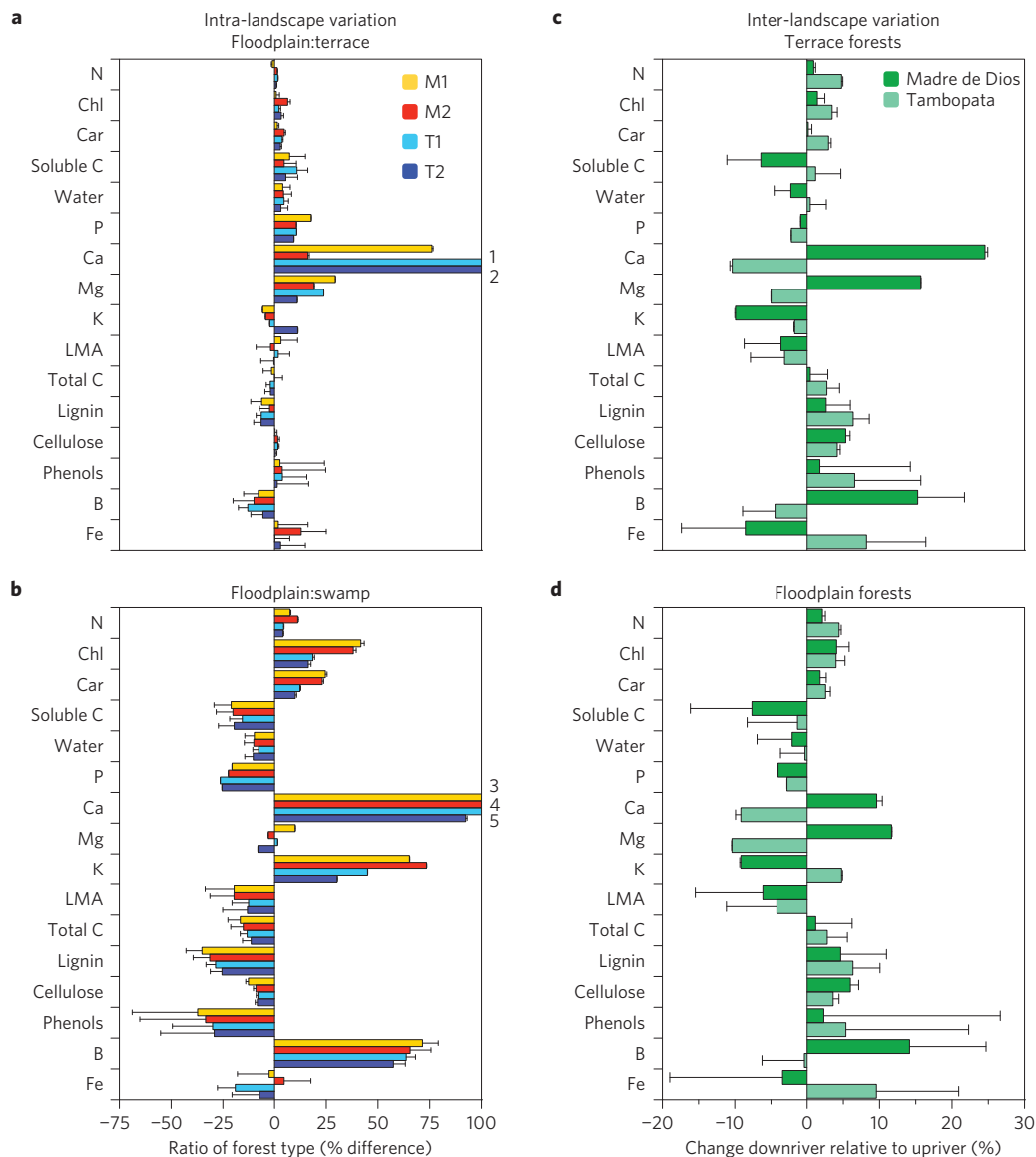


Figure 4 | Intra-landscape and inter-landscape changes in remotely sensed canopy traits in lowland Amazonia. **a,b**, Percentage difference in canopy traits between floodplain and *terra firme* terrace forests (**a**) and floodplain and swamp forests (**b**). **c,d**, Inter-landscape differences in canopy traits for terraces (**c**) and floodplains (**d**) located upriver and downriver. Error bars indicate one standard deviation of canopy traits at one-hectare resolution. Notations to the right of **a,b** are for values that exceed the graphed range: (1) $112.1 \pm 0.5\%$; (2) $117.2 \pm 0.7\%$; (3) $276.8 \pm 0.6\%$; (4) $339.6 \pm 0.7\%$; (5) $118.4 \pm 0.5\%$.

in floodplain forests. All other foliar chemical comparisons show minimal or variable directional change between floodplain and terrace forests. Reasons for the contrasting foliar chemistry between neighbouring terrace and floodplain forests centre on substrate age and deposition frequency. Floodplain substrates usually date only to the Holocene, and are generally nutrient-rich¹⁹. Moreover, they often receive nutrient inputs during the wet season (November to June), with some areas readily inundated with small rainfall events, and others flooded only during major storms²⁰. Terrace surfaces are just metres higher than the floodplains, yet they are older, dating to the Quaternary and the Neogene in some cases²¹. Terraces are depleted in rock-derived nutrients, particularly P, Ca and Mg (ref. 7), relative to neighbouring floodplain soils. As a result, terrace soils harbour trees with suppressed distributions of rock-derived nutrients in their leaves.

Swamp canopy chemical properties are highly divergent from those of terrace and floodplain forests. These swamps are compositionally constrained to near-monotypic stands of *Mauritia flexuosa*

in highly anoxic conditions. Swamp forest canopies maintain lower concentrations of foliar N, Ca, K and B than do their neighbouring floodplain forest canopies. Highly anoxic soils suppress N supply²², which may explain the observed increase in structural and defence allocation to lignin, cellulose and phenols. This suite of chemical traits is also highly conducive to the formation of carbon-rich peat in palm swamp soils. Because these swamps occur in vast portions of western Amazonia²³, they may serve to reduce the functional diversity of the region while greatly boosting belowground carbon stocks.

Signals of shifting nutrient limitation

Whereas terrace and floodplain forests differ locally in terms of foliar rock-derived nutrient concentrations and allocation to lignin, we also found that landscape position along rivers is associated with distributional shifts in multiple functional traits (Fig. 5b). Independent of forest type, leaf P decreases whereas N increases from upriver to downriver landscapes. Opposing trends for N and P result in substantial changes in foliar N:P ratio distributions, which

Table 1 | Relative importance of forest type and landscape position along rivers in determining community-scale changes in forest canopy foliar traits.

	Floodplain and terrace forests			Floodplain, terrace and palm swamp forests		
	Landscape	Forest type	Interaction	Landscape	Forest type	Interaction
Light capture and growth						
Nitrogen	945.9	NS	22.2	108.4	83.6	21.5
Chlorophylls ab	562.7	4.3	5.3	27.4	391.3	31.7
Carotenoids	553.0	12.6	13.2	31.0	352.1	32.5
Soluble C	926.1	130.3	46.5	449.6	1,071.9	28.4
Water	92.3	285.3	41.3	62.5	1,235.2	26.5
Rock-derived nutrients						
P	100.4	333.6	114.5	198.1	1,734.5	65.8
Ca	81.5	445.9	26.6	14.9	738.0	25.3
Mg	279.1	717.8	194.1	86.4	372.2	105.7
K	565.4	NS	169.7	28.9	1,122.9	126.8
Structure and defence						
LMA	1,032.6	18.5	98.6	702.8	2,837.1	149.1
Total C	584.1	67.5	10.8	176.4	2,120.5	27.5
Lignin	364.2	93.4	7.8	161.9	1,950.4	25.3
Cellulose	2,231.0	45.5	48.9	1,469.7	1,583.4	41.1
Phenols	379.3	16.6	15.9	170.4	2,782.2	29.0
Secondary elements						
B	109.7	23.3	44.9	77.5	593.9	26.3
Fe	352.7	7.5	8.6	101.8	23.4	22.3

Results of analyses of variance (F-values) for remotely sensed leaf traits among landscapes, forest types and their interactions. Data are partitioned in floodplain and terrace forests, and repeated with swamps included. All differences were significant ($p < 0.01$) unless indicated as not significant (NS).

markedly increases downriver in all forest types, including palm swamp vegetation (Supplementary Fig. 4). In terms of net primary production (NPP), synthesis studies indicate that foliar N:P values of 14–16 mark an approximate threshold between N-limitation at lower ratios and P-limitation at higher ratios²⁴. The P-poor terrace canopies underwent an increase in N:P of just 9% down both river systems, whereas the P-rich floodplain canopies underwent N:P increases of 18–22% downriver. These trends were driven by larger decreases in foliar P relative to increased N (Supplementary Table 2). This suggests that, as P is mobilized in the Andes and deposited in the lowlands²⁵, it becomes increasingly scarce to the east. Our results also suggest that palaeodepositional surfaces such as terraces, which do not at present receive river-borne nutrient subsidies, also exhibit a pattern of decreasing P availability with distance from the Andes.

We note that the N:P ratio of the extremely N-poor, P-rich swamp canopy foliage also increased by up to 20% downriver (Supplementary Fig. 5). This trend was about equally driven by increasing N and decreasing P in the swamp foliage. In contrast to the terraces and floodplains, however, the N:P ratios of the swamps always fell far below the 14–16 threshold suggestive of N-limitation to growth²⁶. This may be linked to anoxia, suppressed decomposition and low N availability²².

If P availability limits primary production in lowland forests, then decreases in foliar P along rivers should be paralleled by functional trait adaptations that reduce P demand from soils²⁷. Indeed we found that communities located farther downriver with relatively low leaf P also contain higher concentrations of structural and defence compounds (Fig. 5b). Total C, lignin, cellulose and phenols each increased substantially in all forests along rivers. Increased lignin and total C concentrations are a classic response to low soil nutrient supply²⁸, serving as adaptations that increase leaf life span, thereby reducing new foliar construction costs, while ensuring future carbon gain through photosynthesis²⁹. Although LMA decreased and N increased from upriver to downriver landscapes, as per the global leaf economics hypothesis³⁰, we found increasing

structural and defence compound investment with decreasing foliar P (Fig. 5b). Foliar structural responses to P, and not N, are strongly suggestive of rock-derived nutrient limitation dominating the Amazonian lowlands, which increases in strength along rivers flowing towards Brazil⁷.

Overall, these intra- and inter-landscape shifts in multiple canopy chemical traits reveal the sensitivity of forest functioning to microtopography and its associated processes of nutrient mobilization and deposition. Additional fieldwork was undertaken to determine whether these functional trait shifts are mirrored by changing species composition. If so, then plant community turnover (beta diversity) is interconnected with changes in functional trait composition; if not, then phenotypic plasticity probably underpins the patterns we have observed. Our field surveys indicated that only 13%, 2% and 0% of families, genera and species, respectively, were shared among all four landscapes (Supplementary Table 3). Only ten plant families were common to all landscapes. Only 25% and 20% of families were common to all floodplain and terrace forest canopies, respectively. Far fewer genera or species were common to these forest types. Moreover, just 16–27% of families, 2–8% of genera, and <1% of species were common to upriver and downriver landscapes within a river system. These basic compositional patterns suggest that canopy species turnover parallels that of functional trait turnover. These results echo recent field-survey findings of strong phylogenetic control over many canopy chemical traits of Amazonian trees⁸; however, the spatial extent of these patterns and the distribution of canopy traits among them, as reported here, were previously indeterminable. In addition, past field and remote sensing work has indicated pronounced species turnover between floodplain and terrace communities^{5,13}, yet the role of river position in filtering traits was also unknown until now. Taken together, our results suggest that microtopographic variation in canopy chemical trait distributions also expresses changing taxonomic composition, with the most pronounced turnover occurring at both genus and species levels.

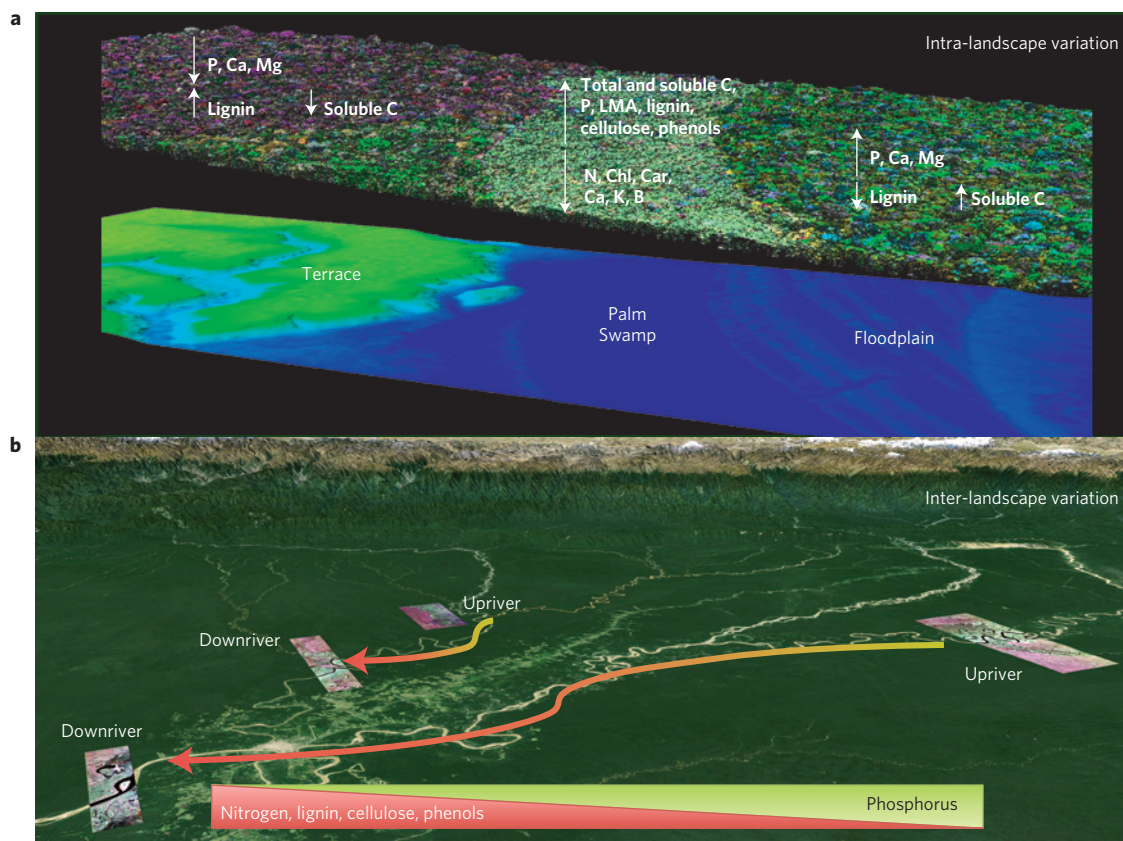


Figure 5 | Intra-landscape and inter-landscape shifts in canopy chemistry along lowland Amazonian rivers. a, Intra-landscape summary of terrace-swamp-floodplain sequences. Forest canopy structure and microtopography are derived from the airborne LiDAR, and the colours indicate community-scale differences in foliar traits derived from airborne imaging spectroscopy. **b**, Inter-landscape summary of the major changes in community-scale chemical traits along lowland Amazonian rivers.

For many years, the scientific community has relied on field collections, often within small plots, and from leaf to leaf or from plant to plant, with the aim of understanding the diversity and assembly of plant communities and ecosystems. Yet there has been no way to assess whether results from field studies are representative of an entire community, a landscape, or a biome. This is particularly true in lowland Amazonian forests containing hundreds of tree and liana species per hectare, and thousands of other species that mediate plant functional trait evolution. To meet this challenge, we developed a new approach based on airborne imaging spectroscopy and LiDAR from the Carnegie Airborne Observatory that provides spatially explicit distributional data on multiple canopy foliar traits at a scale unachievable in field studies. From these measurements, it is possible to map, assess and compare multiple functional trait patterns at many ecological scales, while also resolving the contributory role of the organisms within the system. Landscape- and regional-scale distributions of plant functional traits have not been observed in humid tropical forests. Our findings thus highlight a need for expanded spectroscopic mapping of tropical forest landscapes, with a goal of revealing the inter-connections between biological diversity and biogeochemical processes.

Methods

Methods and any associated references are available in the [online version of the paper](#).

Received 23 November 2014; accepted 20 April 2015;
published online 25 May 2015

References

1. von Humboldt, A. *Aspects of Nature in Different Lands and Different Climates* (Lea and Blanchard, 1850).
2. Tilman, D. Functional diversity. *Encycl. Biodiv.* **3**, 109–120 (2001).
3. Ostle, N. J. *et al.* Integrating plant-soil interactions into global carbon cycle models. *J. Ecol.* **97**, 851–863 (2009).
4. Fine, P. V. A. *et al.* The growth-defense trade-off and habitat specialization by plants in Amazonian forests. *Ecology* **87**, S150–S162 (2006).
5. Asner, G. P. & Martin, R. E. Canopy phylogenetic, chemical and spectral assembly in a lowland Amazonian forest. *New Phytol.* **189**, 999–1012 (2011).
6. ter Steege, H. *et al.* Continental-scale patterns of canopy tree composition and function across Amazonia. *Nature* **443**, 444–447 (2006).
7. Quesada, C. *et al.* Regional and large-scale patterns in Amazon forest structure and function are mediated by variations in soil physical and chemical properties. *Biogeosciences* **6**, 3993–4057 (2009).
8. Asner, G. P. *et al.* Amazonian functional diversity from forest canopy chemical assembly. *Proc. Natl Acad. Sci. USA* **111**, 5604–5609 (2014).
9. *Geological Map of Peru* (Instituto Geológico Minero y Metalúrgico, 2000).
10. Hoorn, C. *et al.* Amazonia through time: Andean uplift, climate change, landscape evolution, and biodiversity. *Science* **330**, 927–931 (2010).
11. Hamilton, S. K., Kellndorfer, J., Lehner, B. & Tobler, M. Remote sensing of floodplain geomorphology as a surrogate for biodiversity in a tropical river system (Madre de Dios, Peru). *Geomorphology* **89**, 23–38 (2007).
12. Rosenqvist, A., Forsberg, B. R., Pimentel, T., Rauste, Y. A. & Richey, J. E. The use of spaceborne radar data to model inundation patterns and trace gas emissions in the central Amazon floodplain. *Int. J. Remote Sensing* **23**, 1303–1328 (2002).
13. Féret, J.-B. & Asner, G. P. Microtopographic controls on lowland Amazonian canopy diversity from imaging spectroscopy. *Ecol. Appl.* **24**, 1297–1310 (2014).
14. Vitousek, P. M. Nutrient cycling and nutrient use efficiency. *Am. Nat.* **119**, 553–572 (1982).
15. Weng, J.-K. & Chapple, C. The origin and evolution of lignin biosynthesis. *New Phytol.* **187**, 273–285 (2010).

16. Coley, P. D., Kursar, T. A. & Machado, J.-L. Colonization of tropical rain forest leaves by epiphylls: Effects of site and host-plant leaf lifetime. *Ecology* **74**, 619–623 (1993).
17. Niinemets, U. & Kull, O. Stoichiometry of foliar carbon constituents varies along light gradients in temperate woody canopies: Implications for foliage morphological plasticity. *Tree Physiol.* **18**, 467–479 (1998).
18. Asner, G. P. *et al.* Carnegie Airborne Observatory-2: Increasing science data dimensionality via high-fidelity multi-sensor fusion. *Remote Sensing Environ.* **124**, 454–465 (2012).
19. Kalliola, R., Puhakka, M., Salo, J., Linna, A. & Räsänen, M. Mineral nutrients in fluvial sediments from the Peruvian Amazon. *Catena* **20**, 333–349 (1993).
20. Kvist, L. P. & Nebel, G. A review of Peruvian flood plain forests: Ecosystems, inhabitants and resource use. *Forest Ecol. Manage.* **150**, 3–26 (2001).
21. Räsänen, M. E., Salo, J. S., Jungner, H. & Pittman, L. R. Evolution of the Western Amazon Lowland Relief: Impact of Andean foreland dynamics. *Terra Nova* **2**, 320–332 (1990).
22. Schuur, E. A. G., Chadwick, O. A. & Matson, P. A. Carbon cycling and soil carbon storage in mesic to wet Hawaiian montane forests. *Ecology* **82**, 3182–3196 (2001).
23. Householder, J. E., Janovec, J. P., Tobler, M. W., Page, S. & Lähteenoja, O. Peatlands of the Madre de Dios River of Peru: Distribution, geomorphology, and habitat diversity. *Wetlands* **32**, 359–368 (2012).
24. Townsend, A. R., Cleveland, C. C., Asner, G. P. & Bustamante, M. M. C. Controls over foliar N:P ratios in tropical rain forests. *Ecology* **88**, 107–118 (2007).
25. Richey, J. E. *et al.* Organic matter and nutrient dynamics in river corridors of the Amazon Basin and their response to anthropogenic change. *Geophys. Res.* **97**, 3787–3804 (1997).
26. Koerselman, W. & Meuleman, A. F. M. The vegetation N:P ratio: A new tool to detect the nature of nutrient limitation. *J. Appl. Ecol.* **33**, 1441–1451 (1997).
27. Killingbeck, K. T. Nutrients in senesced leaves: Keys to the search for potential resorption and resorption efficiency. *Ecology* **77**, 1716–1728 (1996).
28. Melillo, J. M., Aber, J. D. & Muratore, J. F. Nitrogen and lignin control of hardwood leaf litter decomposition dynamics. *Ecology* **63**, 621–626 (1982).
29. Chapin, F. S. III, Vitousek, P. M. & Van Cleve, K. The nature of nutrient limitation in plant communities. *Am. Nat.* **127**, 48–58 (1986).
30. Wright, I. J. *et al.* The worldwide leaf economics spectrum. *Nature* **428**, 821–827 (2004).

Acknowledgements

This study was funded by the John D. and Catherine T. MacArthur Foundation. The Carnegie Airborne Observatory is made possible by the Avatar Alliance Foundation, Margaret A. Cargill Foundation, John D. and Catherine T. MacArthur Foundation, Gordon and Betty Moore Foundation, Grantham Foundation for the Protection of the Environment, W. M. Keck Foundation, M. A. N. Baker and G. L. Baker Jr, and W. R. Hearst III.

Author contributions

G.P.A. designed and secured funding for the study, and led data collection and analysis steps. G.P.A., C.B.A., R.E.M., D.E.K., R.T. and F.S. carried out data collection and analyses. G.P.A. and R.E.M. wrote the paper.

Additional information

Supplementary information is available in the [online version of the paper](#). Reprints and permissions information is available online at www.nature.com/reprints. Correspondence and requests for materials should be addressed to G.P.A.

Competing financial interests

The authors declare no competing financial interests.

Methods

Study landscapes. We worked on four large study landscapes located in the Madre de Dios watershed of the southern Peruvian Amazon (Fig. 1). Despite contrasting hydrographic and edaphic conditions among the four landscapes, each landscape contains low-elevation forests that undergo periodic flooding (floodplains) as well as terraces (*terra firme*) of variable height that are free from flooding. On the upper reaches of many western Amazonian rivers closer to the Andes, these terraces of Pleistocene origin are slightly higher in elevation than those found downriver and farther from the Andes³¹.

The largest study landscape, located at Centro de Investigación y Capacitación Rio Los Amigos (CICRA; M1) at the confluence of Madre de Dios and Los Amigos Rivers, is the farthest upriver (Fig. 1). This landscape is 17,108 ha, and has the highest terraces (16–45 m), creating the largest relief compared to the other study landscapes (Supplementary Table 1). The downriver landscape to CICRA, called Inkaterra (M2), is 4,729 ha and is located 110 km to the east on the Madre de Dios River. Wide floodplains and low terraces of 5–12 m in height characterize this landscape. Two other study landscapes were established on the Tambopata River, located to the south of the Madre de Dios River (Supplementary Fig. 1). The upriver landscape, Chuncho (T1), is 6,033 ha, and has moderately high terraces (13–17 m) neighbouring expansive floodplains (Supplementary Table 1). Finally, the Explorer's Inn (E.I.; T2) landscape is 9,316 ha, located about 40 km downriver from Chuncho, and contains terraces of 4–11 m in height above the neighbouring floodplain.

The terraces in each landscape are characterized by low-fertility ultisol and oxisol soils, whereas floodplains contain alluvial inceptisols of much higher fertility. The frequency, extent and depth of flooding in each floodplain portion of the four landscapes are unknown. In addition to the floodplain–terrace dichotomy, the floodplains often vary subtly in relief, and include anoxic swamp areas 2–3 m lower than the average floodplain elevation (Supplementary Table 1). These swamp forests are dominated by the palm tree species *Mauritia flexuosa* (Arecaceae).

Airborne data. Airborne remote sensing data were acquired in August–September 2013 using the Carnegie Airborne Observatory (CAO), which includes a high-fidelity imaging spectrometer (HiFIS) and a dual laser, waveform LiDAR (ref. 18). The CAO data were acquired over each study landscape from an altitude of 2,000 m above ground level (a.g.l.), an average flight speed of 55–60 m s⁻¹, and a mapping swath of 1,200 m. The HiFIS measures spectral radiance in 480 contiguous channels spanning the 252–2,648-nm wavelength range in 5-nm increments (full-width at half-maximum) at a frame rate of 10 ms. The HiFIS has a 34° field-of-view and an instantaneous field-of-view of 1 mrad. At 2,000 m a.g.l., the data collection provided a 2.0 m ground sampling distance (pixel size) across- and down-track, throughout each study landscape. The LiDAR has a beam divergence set to 0.5 mrad, and was operated at 200 kHz with a 17° scan half-angle from nadir, providing swath coverage similar to the HiFIS. Because the airborne data were collected along adjacent flightlines with 50% overlap, the LiDAR point density was two laser shots m⁻², or eight shots per HiFIS pixel.

Pre-processing of remotely sensed data. CAO LiDAR laser ranges were combined with the embedded high-resolution global positioning system–inertial measurement unit (GPS-IMU) data to determine the 3D locations of laser returns, producing a 'cloud' of LiDAR data. The LiDAR data cloud consists of a very large number of georeferenced points, which are quantified in elevation (cm) relative to a reference ellipsoid (WGS 1984). We used these points to create an interpolated raster digital terrain model (DTM) for the ground surface of each landscape. This was achieved using a 10 m × 10 m kernel passed over each flight block; the lowest elevation estimate in each kernel was assumed to be ground. Subsequent points were evaluated by fitting a horizontal plane to each of the ground seed points. If the closest unclassified point was <5.5° and <1.5 m higher in elevation, it was classified as ground. This process was repeated until all points within the block were evaluated. A digital surface model (DSM), defining the outermost layer of the data, was created based on interpolations of all first-return points. Measurement of the vertical difference between the DTM and DSM yielded a digital canopy model (DCM) of vegetation height above ground.

The HiFIS data were radiometrically corrected from raw digital number (DN) values to radiance (W m⁻² sr⁻¹ nm⁻¹) using a flat-field correction, radiometric calibration coefficients and spectral calibration data collected in the laboratory. GPS pulse-per-second measurements, a camera model, and LiDAR DCM were used to precisely co-locate the HiFIS spectral and LiDAR data, and to generate data on the solar and viewing geometry for each HiFIS image pixel¹⁸. These inputs were used to atmospherically correct the radiance imagery using the ACORN-5 model (ImSpec LLC). We convolved the HiFIS reflectance spectra to 10-nm bandwidth and applied a brightness-normalization adjustment. Brightness normalization reduces the contribution of varying LAI to chemometric determinations of foliar traits from remotely sensed data³². The spectra were trimmed at the far ends (<410 nm, >2,450 nm), and in atmospheric water vapour channels (1,350–1,480, 1,780–2,032 nm).

Chemical mapping. The technique for mapping of canopy chemical traits and LMA was developed and validated in ref. 33. Given its importance in this study, we describe the method here and provide summary evidence for its performance. The method generates spectral data sets at 1-ha mapping resolution while minimizing the local-scale effects of illumination and viewing angle variation, crown architecture, inter- and intra-crown shading, forest gaps, and terrain-related artefacts. To achieve this goal, we used a data-fusion approach facilitated by a combination of co-aligned HiFIS and LiDAR data. The HiFIS data were processed in 1-ha grid cells, and the spectral signature of the 1-ha cell was derived by averaging the 2-m resolution spectra of all HiFIS measurements that passed a series of filters in each 1-ha grid cell (Supplementary Fig. 5). These filters included normalized difference vegetation index (NDVI) > 0.8, vegetation height > 2.0 m, no detectable intra- or inter-canopy shade, no cloud and cloud-shadow, and no land clearings (land use). A minimum NDVI threshold of 0.8 was conservative as it allowed most canopy foliage into the spectral analysis, while excluding portions of unfoliated canopy. The minimum vegetation height requirement removed bare ground, short vegetation such as exposed grass cover and land clearings. The shade mask was derived from a ray tracing model that precisely identifies canopy location in an unshaded and unobstructed view of the HiFIS (ref. 34). This filtering approach has the unique advantage of reducing the total canopy analysis area to a level analogous to the 'sunlit canopy foliage' criterion often used in field collections of forest canopy foliage. A previous calibration and validation study indicated that an average 52% (5,200 m²) of canopy was sampled in each mapping hectare (10,000 m²), providing a highly robust sampling of canopies while minimizing noise from poorly illuminated and/or non-canopy surfaces³³.

Following the preparation of the 1-ha averaged HiFIS spectra, we used chemometric equations derived from a previously performed calibration–validation study³³ to map 15 chemical traits and LMA at 1-ha resolution throughout each study landscape. We used partial least squares regression (PLSR; ref. 35) to calibrate the HiFIS spectra to field-collected, lab-assayed foliar traits³⁶. PLSR involves dimensionality reduction of spectral information to orthogonal synthetic latent vectors (similar to PCA) containing the maximum explanatory power in relation to the chemical data, thus overcoming problems caused by spectral collinearities and small sample sizes³⁷. To minimize statistical over-fitting, the number of latent vectors used in the PLSR analysis was estimated by minimizing the prediction residual error sum of squares (PRESS) statistic³⁸. We calibrated the 1-ha resolution HiFIS spectra to 16 canopy foliar traits, with spectral weightings shown in Supplementary Fig. 6. A detailed report on the calibration, along with a validation in 79 one-hectare plots across western Amazonia, is provided in ref. 33. Calibration results indicate the strength of the link between the 1-ha HiFIS spectra and the foliar traits estimated in the field (Supplementary Table 4). All results are reported as remotely sensed foliar traits.

Elevation and community classification. We required an objective method to classify terrain throughout the four study landscapes in a way that preserves their internal (within-community) microtopographic variation, while also separating more substantial changes in local terrain associated with floodplain and terrace surfaces. These two geomorphological classes can be readily identified when terraces end with an abrupt edge, such as in the upriver landscapes, but it is more challenging when floodplains alternate with terraces having 'soft' edges common to the downriver sites. To address this issue, we converted absolute elevation derived from airborne LiDAR to relative elevation. Relative elevation was defined as the change in height relative to major rivers, such that lower elevation surfaces, which may be regularly flooded, are classified as floodplains and higher elevation surfaces are classified as terraces. The first step to obtain relative elevation was to define an isosurface corresponding to major streams. For the isosurface, data from the NASA Shuttle Radar Topography (SRTM) was used to identify major rivers and measure their elevation. For each site, the isosurface was subtracted from the LiDAR digital terrain models to obtain relative elevation values (Supplementary Table 1).

In addition to the elevation modelling, we also manually delineated large patches of vegetation dominated by *Mauritia flexuosa*, the most common palm species found in the western Amazonian lowland³⁹. *M. flexuosa* occurs mostly in young to medium aged swamp areas that were formerly oxbow lakes and/or portions of neighbouring meandering rivers. Because *M. flexuosa* has such a distinct structure, it was readily observed in the VSWIR imagery, which was confirmed using high-resolution images in Google Earth.

Statistical analyses. All populations of remotely sensed leaf traits were close to normally distributed (Fig. 3 and Supplementary Figs 2 and 3). Transformation did not improve normality and was not implemented. Standard least squares analysis of variance (ANOVA) with Tukey HSD (Honestly Significant Difference) *post hoc* tests were used to assess differences in remotely sensed leaf traits among population means on different landscapes, in different forest types and any interaction between these factors. Kolmogorov–Smirnov comparisons were performed in a pairwise fashion to assess whether the shapes of remotely sensed canopy foliar trait distributions varied among forest type and/or location. Landscape- and

regional-scale changes in chemical leaf traits were compared in terms of relative differences. The percentage difference in traits between floodplain (FP) and *terra firme* forests (TF); and floodplain and palm swamp forest (PS) was calculated as $[100 \times (FP/(TF \text{ or } PS) - 100)]$. The variation was propagated as $\sigma_{FP/TF \text{ or } PS} = \sqrt{(\sigma_{FP}^2 + (\sigma_{TF \text{ or } PS})^2)}$. Change in traits within a forest type between upriver and downriver positions was calculated as $100 \times (\text{downriver} - \text{upriver})/(\text{downriver} + \text{upriver})$. The variation was propagated as $\sigma_{\text{down/up}} = \sqrt{(\sigma_{\text{down}}^2 + \sigma_{\text{up}}^2)}$. All statistical analyses were carried out using the SAS JMP 10.0 statistical software package (SAS Institute).

Field surveys. We surveyed canopy tree and liana composition in each floodplain and terrace forest on the four study landscapes. The goal was to be as comprehensive as possible at the scale of each floodplain and terrace surface within each landscape. Our sampling strategy focused on exhaustive surveys of as many sunlit canopy species, both common and rare, as possible over forest community areas of 300–600 ha, broadly directed by historical surveys from the same or similar locations. Individual canopies meeting the fully sunlight criterion were marked and a voucher specimen was collected. Vouchers were matched by Carnegie Institution taxonomists to type specimens kept at the National Agrarian University La Molina Herbarium in Peru and the Missouri Botanical Garden. We also matched genus names to information provided by Kew Botanical Gardens. A total of 1,673 individuals in 625 canopy species were recorded in all landscapes. Depending on forest type and landscape location, we found 46–227 species in 35–135 genera in 25–56 families per study forest (Supplementary Table 5).

Data availability. Remotely sensed data associated with the findings of this paper are available on request. The data request should be directed to G.P.A.

References

- Nikitina, D., Remizova, L. & Losco, R. L. A preliminary investigation of the soils and geomorphology of a portion of the Madre de Dios Region, Peru. *Soil Surv.* **52**, 40–47 (2011).
- Feilhauer, H., Asner, G. P., Martin, R. E. & Schmidlein, S. Brightness-normalized partial least squares regression for hyperspectral data. *J. Quant. Spectrosc. Radiat. Transfer* **111**, 1947–1957 (2010).
- Asner, G. P., Martin, R. E., Anderson, C. B. & Knapp, D. E. Quantifying forest canopy traits: Imaging spectroscopy versus field survey. *Remote Sensing Environ.* **158**, 15–27 (2015).
- Asner, G. P. *et al.* Carnegie airborne observatory: In-flight fusion of hyperspectral imaging and waveform light detection and ranging for three-dimensional studies of ecosystems. *J. Appl. Remote Sensing* **1**, 013536 (2007).
- Haaland, D. M. & Thomas, E. V. Partial least-squares methods for spectral Analyses. 1. Relation to other quantitative calibration methods and the extraction of qualitative information. *Anal. Chem.* **60**, 1193–1202 (1988).
- Asner, G. P. *et al.* Spectroscopy of canopy chemicals in humid tropical forests. *Remote Sensing Environ.* **115**, 3587–3598 (2011).
- Wold, S., Sjostrom, M. & Eriksson, L. PLS-regression: A basic tool of chemometrics. *Chemometr. Intell. Lab. Syst.* **58**, 109–130 (2001).
- Chen, S., Hong, X., Harris, C. J. & Sharkey, P. M. Sparse modeling using orthogonal forest regression with PRESS statistic and regularization. *IEEE Trans. Syst. Man Cybern.* **34**, 898–911 (2004).
- Goodman, R. C. *et al.* Amazon palm biomass and allometry. *Forest Ecol. Manage.* **310**, 994–1004 (2013).